THE JOURNAL OF PHYSICAL CHEMISTRY B

Article

pubs.acs.org/JPCB

Molecular Dynamics Simulations for Complexation of DNA with 2 kDa PEI Reveal Profound Effect of PEI Architecture on Complexation

Chongbo Sun,[†] Tian Tang,*[,†] and Hasan Uludağ[‡,§,∥]

[†]Department of Mechanical Engineering, University of Alberta, Edmonton, Canada

[‡]Department of Chemical and Materials Engineering, University of Alberta, Edmonton, Canada

[§]Department of Biomedical Engineering, University of Alberta, Edmonton, Canada

[∥]Faculty of Pharmacy and Pharmaceutical Sciences, University of Alberta, Edmonton, Canada

Supporting Information

ABSTRACT: A series of all-atom molecular dynamics (MD) simulations of the complexation between DNA and 2 kDa branched and linear polyethylenimines (PEIs) are reported in this study. The simulations revealed distinct binding modes of branched and linear PEIs to DNA, with branched PEIs adhering to the DNA surface like beads and linear PEIs adhering to the DNA surface like cords. The dynamics of each PEI's binding state to the DNA during the simulations and how the PEIs neutralize the DNA were quantified. For both branched and linear PEIs, the addition of salt ions similar to physiological conditions were found to have only a small effect on DNA/PEI complexation compared to salt-free conditions. The simulation results reported here will be helpful to understand the mechanism of action for the PEI-based gene carriers.

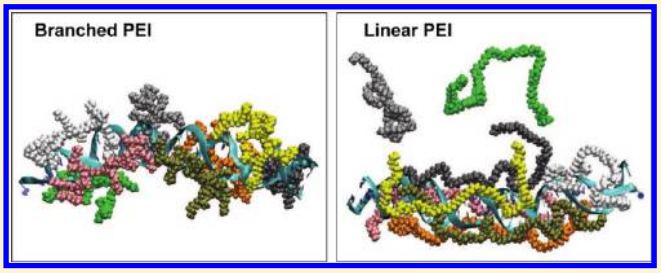

1. INTRODUCTION

Complexation between DNA and synthetic polycations has drawn great interest due to the applications of synthetic polycations as gene carriers.[1,2] Among the polycations, polyethylenimine (PEI) is one of the most effective synthetic molecules serving as gene carriers.[3,4] It can condense nucleic acids into nanoparticles, which can facilitate the cellular uptake of nucleic acids and protect the nucleic acids from degradation during the delivery process. It was found that the efficacy of PEI as a gene carrier depends on the structure and molecular weight of the PEI.[5,6] High molecular weight (HMW) PEIs (i.e., >25 kDa) are more efficient in DNA delivery but also display high cytotoxicity. On the contrary, low molecular weight (LMW) PEIs (e.g., 1−5 kDa) display low cytotoxicity but are also less efficient. Modifying LMW PEIs, for example, through lipid substitution[7,8] or disulfide cross-linking,[9] can overcome the limitations of DNA delivery efficiency. PEI of 2kDa, in particular, is a good platform for such modifications, and some modified 2 kDa PEIs have been proved to be as effective as or even more effective than 25 kDa PEIs for gene transfection.[10,11] It is therefore of great interest to investigate the binding of LMW PEIs to DNA in order to elucidate their roles in the delivery process.

Commercial PEIs have a large structural diversity and are usually categorized into two basic forms, linear and branched. Linear PEIs (lP) are composed of almost all secondary amines, while branched PEIs (bP) consist of primary, secondary, and tertiary amines. Both lP and bP have been adopted in gene delivery and transfection studies.[6,12−15] Experiments on transfection using lP and bP showed that the structural difference could affect the transfection efficiency and sometimes to a significant degree.[6,12−15] However, there has not been a clear conclusion as to whether lP or bP is more effective as gene carriers. Experimental efforts have also been made to elucidate the relationship between transfection and PEI/DNA complexation. Itaka et al. investigated the intracelluar trafficking and DNA release of lP and bP formed polyplexes.[13] They found that the bP/DNA polyplexes were more stable and the DNA could be kept in a condensed state even after 24 h, while lP/DNA polyplexes could be quickly decondensated and yield a considerably higher and faster gene expression. Their atomic force microscopy results also revealed more effective condensation of DNA by bP than by lP, supporting the restricted release of DNA from bP/DNA polyplexes. Dai et al. recently studied the complexation, decondensation, transfection efficiency, and cellular uptake of lP/DNA and bP/DNA polyplexes at different N/P ratios.[15] Their results further confirmed the higher capacity of bP in condensing DNA and the better capacity of lP in releasing DNA from the polyplexes. Despite these experimental findings, the underlying mechanism of the structure−function relationship for PEI-based carriers remains to be probed at the atomistic level.

To understand the role of carrier molecules and to design more effective PEI-based gene carriers, it is crucial to gain a

Received: December 6, 2011
Revised: January 25, 2012
Published: January 31, 2012

   dx.doi.org/10.1021/jp211716v | J. Phys. Chem. B 2012, 116, 2405−2413

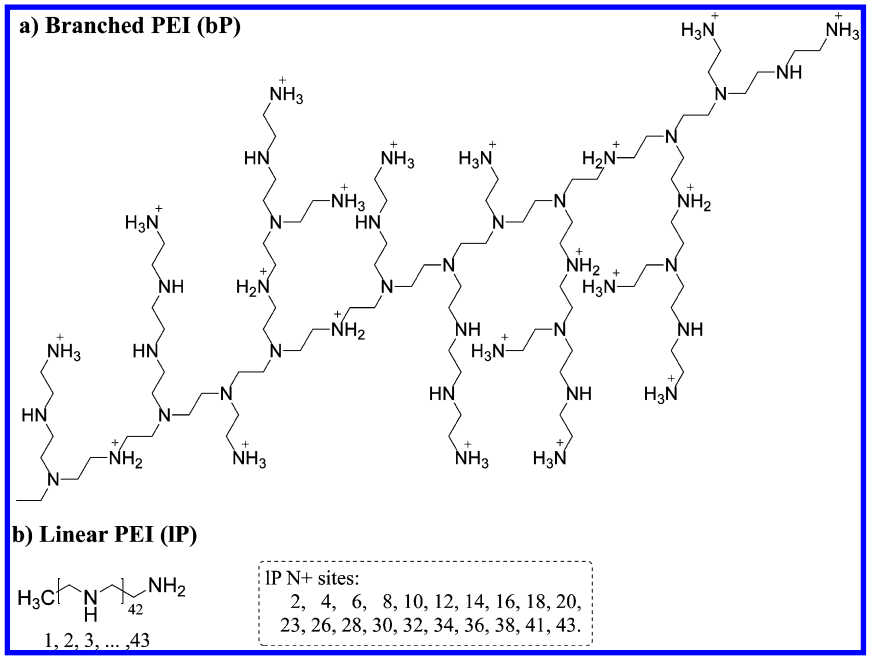

Figure 1. Molecular structure and protonation sites of the PEIs studied: (a) bP and (b) lP.

detailed understanding of the complexation of DNA with PEIs at the atomistic level. With the fast growing computational capacity, simulating the complexation of nucleic acids and polycations in all-atom representation is becoming feasible. For example, Ziebarth et al.[16] simulated the complexation of DNA with linear PEIs (900 and 1700 Da) and compared it with the complexation between DNA and poly-L-lysine. They found that DNA remained in the B form in the DNA/PEI complex, the charged PEI amines mainly interacted with the DNA phosphate groups, and PEI had a higher capability in neutralizing DNA than poly-L-lysine. Pavan et al. reported a series of molecular dynamics (MD) simulations on the complexation of DNA with dendrimers including PAMAM, UV-degradable dendrons, and triazine dendrimers.[17−20] The simulation results showed that the flexibility of dendrimers and their ability to reorganize their structures to comply with DNA structure were important for binding affinity. The complexation of DNA with 600 Da PEIs of different architecture and protonation state was explored in a recent work.[21] It was found that the protonation state of the PEI greatly affected the PEI's complexation with the DNA. In particular, the binding for 46% protonated PEIs was achieved mainly through direct interaction between the protonated amines on the PEI and the electronegative oxygens on the DNA backbone. For the 23% protonated PEIs, however, indirect interaction mediated by water molecules played an important role in binding. Four PEI architectures were simulated with increasing degree of branching, but no strong influence was found on the complexation of these LMW PEIs with the DNA. The above studies have demonstrated the power of atomistic simulations in investigating complexation of nucleic acids with polycations and revealed important details that are not readily accessible by experimental techniques.

In this work, we performed a series of large scale all-atom MD simulations to study the complexation of DNA with 2 kDa PEIs. How the PEI's architecture might influence its complexation with the DNA is a main focus of this study. While previous MD results[21] demonstrated insignificant effects of branching for LMW (600 Da) PEIs, our simulations below for two 2 kDa PEI molecules with different architectures (representing a lP and a bP, respectively) show that the scenario is considerably different. Experimentally, the existence of free PEIs at high N/P ratios has been shown to contribute to cellular uptake and transfection.[15,22] This underlines the importance of incorporating different PEI/DNA ratios in the simulations. In our simulations for both lP and bP, we have used two PEI/DNA and hence two N/P ratios. For transfection purposes, the DNA/PEI complexes are usually prepared without salt or with 154 mM NaCl to mimic physiological osmolarity. For both the lP and bP, we performed simulations at both zero and 154 mM salt concentrations. Our results reveal the different binding characteristics of lP and bP in binding to DNA and the effect of salt concentration on the complexation.

2. METHODS

2.1. Simulated Systems and Procedure. The DNA simulated is a 3-fold Drew-Dickerson dodecamer d-$((CGCGAATTCGCG)_3)$ composed of 72 nucleotides carrying a total charge of −70 in the fully deprotonated state. The initial structure of the DNA was built to be a canonical B form using the AMBER NAB tool.[23] Two types of PEIs in branched and linear forms were simulated, each consisting of 43 amine groups with a molecular mass of 1874 Da. The chemical structures and protonation sites of the two PEIs are shown in Figure 1. Twenty amine groups were chosen to be protonated for each PEI type, corresponding to a protonation ratio of 47% on experimentally determined value at pH = 6.[24] The protonation sites were assigned to only the primary and secondary amines and were arranged as uniformly as possible to minimize thermodynamic interactions among the protonated amines. An MD simulation was first performed for each PEI with explicit water and 20 Cl^- counterions. The structure of each PEI at the end of the simulation was adopted as the initial configuration for PEIs in the complex formation simulations.

Eight systems were simulated to study the complexation of the DNA with multiple PEIs, four of which contain one DNA and four PEIs (DNA/PEI number ratio = 1/4) and the other

dx.doi.org/10.1021/jp211716v | J. Phys. Chem. B 2012, 116, 2405−2413

Table 1. Information of the 10 Systems Simulated

system name	number of DNA/PEI	N/P ratio	charges of DNA/PEI	number of atoms	size of simulation box (Å^3)	ion (mM)	simulation time restrained + free (ns)
bP	0/1	N/A	0/20	37 160	58 × 69 × 92	0	0.2 + 50
D-4bP	1/4	2.5	70/80	131 789	88 × 93 × 158	0	4 + 200
D-4bP-S	1/4	2.5	70/80	131 297	88 × 93 × 157	154	50 + 200
D-8bP	1/8	5	70/160	130 321	88 × 93 × 157	0	4 + 200
D-8bP-S	1/8	5	70/160	129 841	88 × 93 × 157	154	50 + 200
lP	0/1	N/A	0/20	215 834	123 × 150 × 117	0	0.2 + 100
D-4lP	1/4	2.5	70/80	131 666	88 × 93 × 158	0	4 + 200
D-4lP-S	1/4	2.5	70/80	131 174	88 × 93 × 157	154	50 + 200
D-8lP	1/8	5	70/160	130 039	88 × 93 × 157	0	4 + 200
D-8lP-S	1/8	5	70/160	129 559	88 × 93 × 157	154	50 + 200

four contain one DNA and eight PEIs (DNA/PEI number ratio = 1/8). They correspond to N/P ratios (ratio of the total number of N atoms on PEIs to the number of DNA phosphates) of ∼2.5 and ∼5, respectively. At each DNA/PEI number ratio, the two PEI architectures and two salt concentrations (0 and 154 mM) were simulated. The information on the eight systems, together with the two systems involving individual PEIs is summarized in Table 1. In the remaining part of this article, each system will be referred by its name in the first column of Table 1. The systems with 154 mM salt are designated with -S in their names to be distinguished from the systems with zero salt. In systems D-4bP, D-4bP-S, D-4lP, and D-4lP-S, the DNA/PEI charge ratio is 7/8; in systems D-8bP, D-8bP-S, D-8lP, and D-8lP-S, the DNA/PEI charge ratio is 7/16. An overall cationic charge is chosen for the DNA/PEI complexes since that better represents the charge of complexes used for experimental purposes. For the zero salt simulations, only neutralizing Cl^- ions were added to account for the difference between DNA and PEI charges. At the salt concentration of 154 mM, additional Na^+ and Cl^- ions of equal amount were added to the solution, and only these additional ions were counted in the calculation of salt concentration. In constructing the initial configurations for each of the eight systems involving complex formation, the principal axes of the PEIs were initially aligned parallel to the DNA axis, and the center of mass (COM) of each PEI was positioned at 25 Å away from the DNA axis. Detailed arrangement of the initial configurations are illustrated in Figure 2.

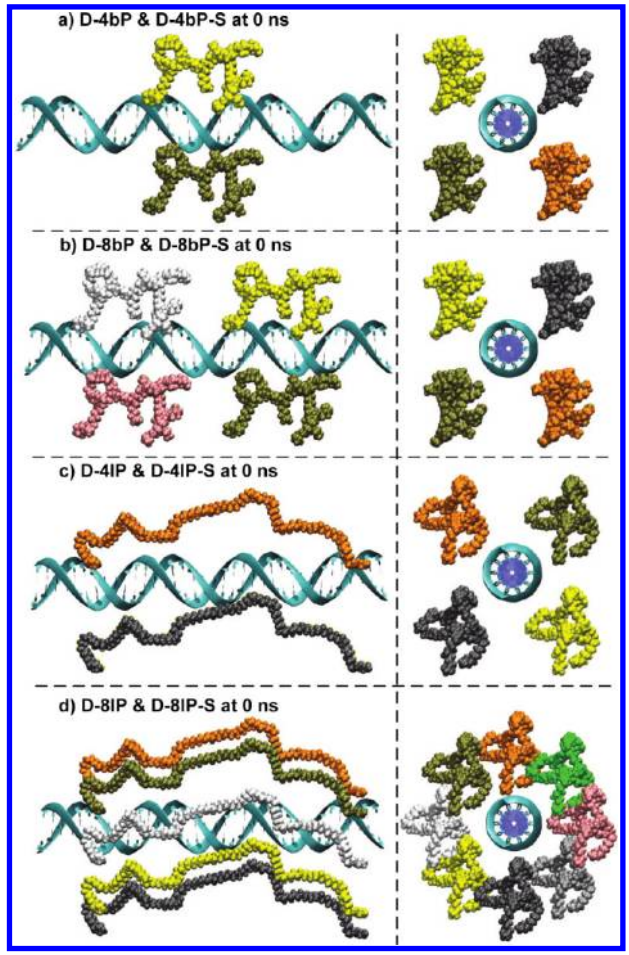

Figure 2. Initial configurations of the systems: (a) D-4bP and D-4bP-S; (b) D-8bP and D-8bP-S; (c) D-4lP and D-4lP-S; and (d) D-8lP and D-8lP-S. Left pane, side view; right panel, axis view. Different PEIs are represented in different colors; water and ions are removed for clarity. Note that because all the PEIs in each model have identical initial configurations, when viewed from a particular direction, some of the PEI molecules may be covered by other PEIs and thus are not visible in certain subfigures.

2.2. Simulation Details. CHARMM 27 force field[25,26] was used for all molecules except for the PEIs as the force field for PEI is not available in CHARMM. A CHARMM format force field was devised for the PEIs based on the CHARMM General Force Field,[27] which has been validated through ab initio calculations, a study on sensitivity of MD results to torsional parameters, and comparison with previous works.[21] All simulations were performed using the MD package NAMD.[28] TIP3P water model,[29] periodic boundary condition, full electrostatics with particle-mesh Ewald method,[30] cutoff distance 10 Å for van der Waals interactions and electrostatics pairwise calculations, SHAKE algorithm[31] to constrain all bonds containing hydrogens, and a time step of 2 fs were used for all of the simulations.

For each system, the DNA and PEIs were solvated into a water box, the size of which is large enough so that the solutes are at least 36 Å away from their nearest periodic images in each direction. Cl^- ions to neutralize the system and NaCl salt ions for the systems in 154 mM salt concentration were then added to the water box by randomly replacing an equivalent amount of water molecules using VMD.[32] During each simulation, the system was first minimized for 5000 steps, then heated from 0 to 300 K in 20 ps with 10 kcal/mol Å^2 harmonic restraint on the nonhydrogen atoms of the solute. The restraint was kept on for a specific period (0.2 ns for bP and lP, 4 ns for the four complex formation simulations with

dx.doi.org/10.1021/jp211716v | J. Phys. Chem. B 2012, 116, 2405−2413

zero salt, and 50 ns for the four complex formation simulations with 154 mM salt) at 300 K and 1 bar to relax the ions around the solutes. The restraint was kept longer for systems with larger amounts of ions to allow them to relax. The restraint was then removed and NPT ensemble simulation was performed for 50 ns for bP, 100 ns for lP, and 200 ns for complex formation simulations. A total length of 1966.6 ns trajectory was generated from the 10 simulations. VMD[32] was used for visualization and trajectories analysis.

3. RESULTS AND DISCUSSIONS

3.1. PEI Flexibility. Figure 3 shows the radii of gyration, R_g, of the bP and lP in the single PEI simulations. It can be seen

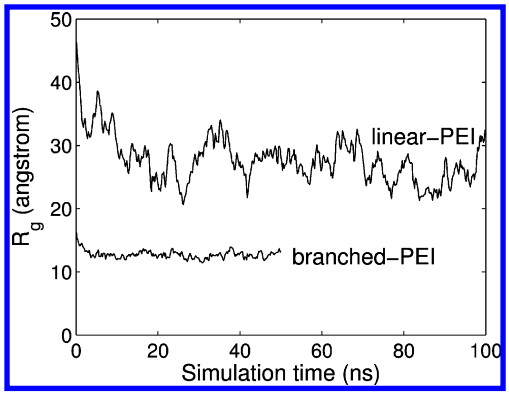

Figure 3. Radius of gyration of the PEIs as a function of simulation time.

that bP has a much smaller R_g (~12 Å) than lP. This is expected as the atoms in the branched PEI are distributed closer to its center of mass in a dendritic manner. In addition, R_g of bP remains almost constant during the entire 50 ns of the simulation, which implies that the bP molecule undergoes very little deformation in the simulation. This is a result of both the inflexible dendritic structure of bP and the fact that each PEI N^+ in bP is closely surrounded by several other PEI N^+, and hence, any large configurational change from the equilibrated structure will introduce a significant energy penalty. On the contrary, R_g of lP fluctuates significantly during the 100 ns simulation, demonstrating the high flexibility of lP.

The flexibility of polycations is known to play important roles in their binding with DNAs and RNAs.[17,18,20] Through MD simulations, Pavan et al. showed that the flexibility of dendrimers and their ability to reorganize their structure for interactions with siRNA significantly affect the binding affinity.[18] They found that rigid dendrimers can reorganize their peripheral groups to generate a larger number of contacts to the nucleic acid and display higher affinity than flexible dendrimers.[20] As will be seen in the subsections below, by studying the dynamics of the PEI/DNA complexation, we also observed distinct binding configurations for linear and branched PEIs, which mainly resulted from the difference in flexibility.

3.2. Dynamics of the Complex Formation. By visually examining the simulation trajectories, we found that for the 4 systems with one DNA and four PEIs, all the PEIs move toward the DNA swiftly during the initial several nanoseconds after the restraint is removed and each PEI established significant contacts with the DNAs within 20 ns. For the 4 systems with one DNA and eight PEIs, the speed of the PEIs moving toward the DNA was slightly slower. In systems D-8bP and D-8bP-S, all PEIs established significant contacts with the DNA within 20 ns, while in systems D-8lP and D-8lP-S, some PEIs did not bind to the DNA even at the end of the simulation. Figure 4 shows the configurations of the eight systems at the final stage of the simulations. It can be seen that for systems D-4bP, D-4bP-S, D-8bP, D-8bP-S, D-4lP, and D-4lP-S, all the PEIs bind to the DNA with a significant part of the molecules complying with the DNA. However, the scenario for systems D-8lP and D-8lP-S was different. In D-8lP, two PEIs have only a small fraction of the molecules in contact with the DNA, and in D-8lP-S, two PEIs are completely separated from the DNA.

To quantify the dynamics of the interaction of PEIs with the DNA, we plotted the binding state of individual PEIs to the DNA in terms of the number of Ns from each PEI in close contact with the DNA (i.e., within 4 Å of any N/O atoms of the DNA) as a function of simulation time. Four angstroms was chosen as the cutoff distance because this is the distance within which a PEI amine group can form a direct hydrogen bond with a DNA.[21] Figure 5 summarizes the results for the four systems with 4 PEIs and Figure 6 for the four systems with 8 PEIs. Figures 5 and 6 also provide the numbers of Ns from all the PEIs that are in close contact with the DNA. Each subfigure in Figures 5 and 6 contains two curves associated with different salt concentrations. In Figure 5, each curve in the top 8 subfigures corresponds to one of the 4 PEIs in a particular system. Each curve in the bottom 2 subfigures describes the total number of Ns of all the 4 PEIs in close contact with the DNA in a particular system. Similarly, in Figure 6, each curve in the top 16 subfigures corresponds to one of the 8 PEIs in a particular system, and each curve in the bottom 2 subfigures corresponds to all the 8 PEIs in a particular system.

The first observation from Figures 5 and 6 is that the two curves in each subfigure have a very similar trend, demonstrating that the ion concentration plays a negligible role in affecting the dynamics of PEIs' binding with the DNA. Second, at the DNA/PEI charge ratio of 7/8 (Figure 5), all the PEIs in each system move toward the DNAs quickly in the first 20 ns reflected by the rapid increase in the number of PEI Ns in close contact with the DNA. The curves for all PEIs stabilize at ~50 ns for bP and at ~25 ns for lP, demonstrating the faster kinetics of lP in binding with the DNA. Each lP has about 18 Ns in close contact with the DNA, which is 50% more than that for bP (~12). This can be explained by the higher flexibility of lP, which allows it to comply more easily with the DNA. In contrast, the rigid dendritic bP can only have part of its molecules facing the DNA to form close contact, and the rest stays away from the DNA so as to avoid significant configurational changes (see Figure 4a–d). In addition, the curves for each lP fluctuate more than that for the bPs. This can again be attributed to the higher flexibility of lP, which make its contacts with the DNA change more frequently.

At the DNA/PEI charge ratio of 7/16, from the final configurations shown in Figure 4c,d,g,h, the DNAs seem to be saturated with their surfaces fully covered by PEIs. This situation is reflected in Figure 6 as we see a competition among the PEIs for binding to the DNAs. Specifically, for systems D-8bP and D-8bP-S, all the 8 PEIs bind to the DNA through the entire simulation, but each PEI has fewer Ns (~9) in close contact with the DNA compared with systems D-4bP and D-4bP-S (~12). For systems D-8lP and D-8lP-S, the competition is more intense, and some PEIs lose contact with the DNA during the simulation or do not have close contact with the

dx.doi.org/10.1021/jp211716v | J. Phys. Chem. B 2012, 116, 2405–2413

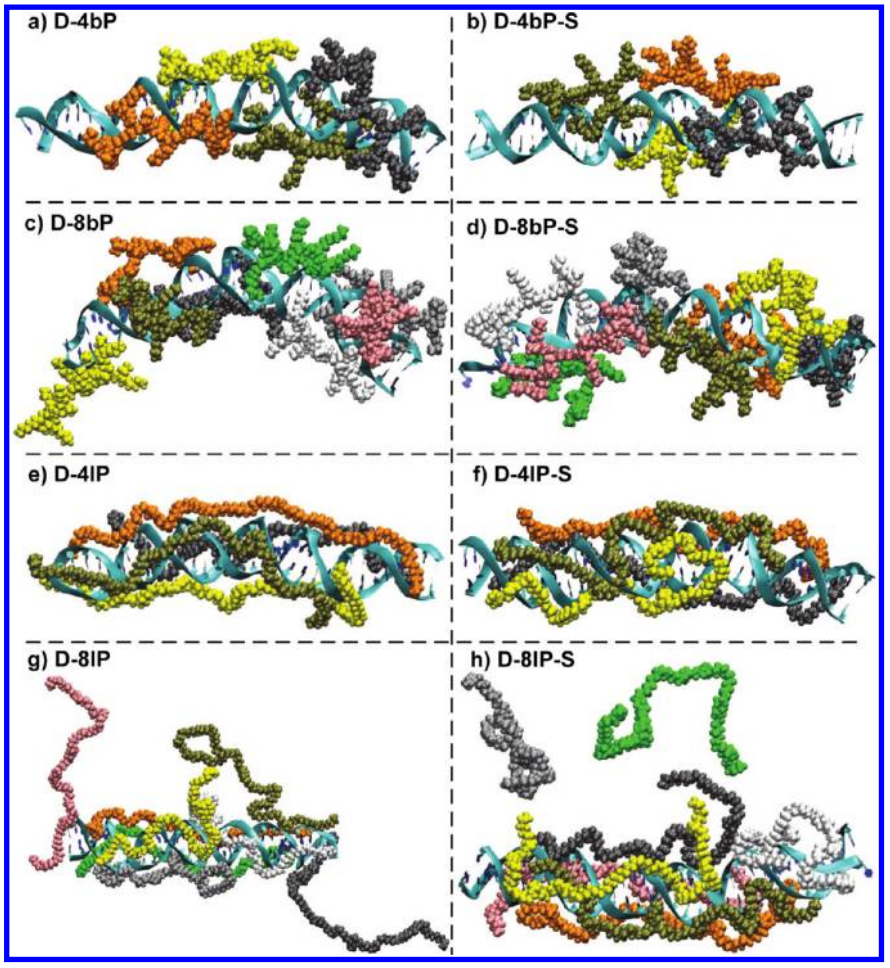

Figure 4. Snapshots of the systems at the final stage of the simulations: (a) D-4bP, (b) D-4bP-S, (c) D-8bP, (d) D-8bP-S, (e) D-4lP, (f) D-4lP-S, (g) D-8lP, and (h) D-8lP-S. Different PEIs are represented in different colors; water and ions are removed for clarity.

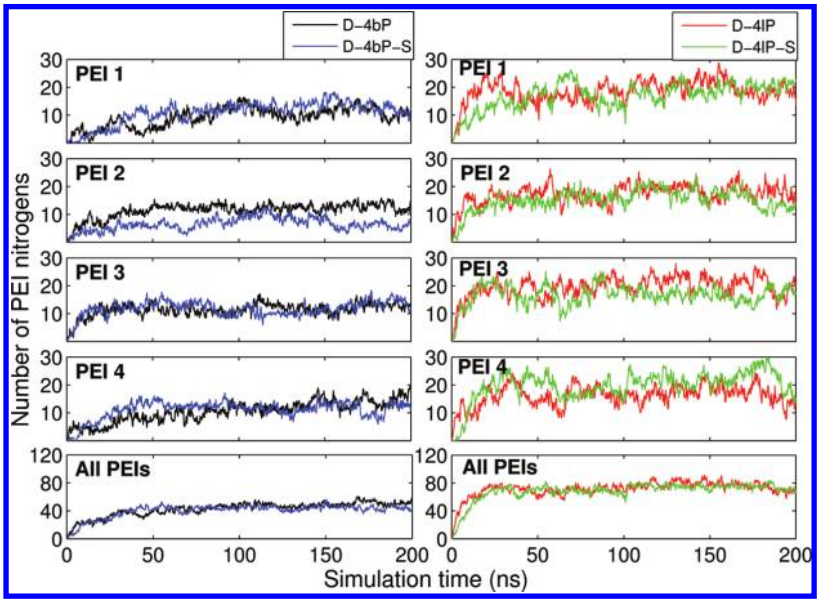

Figure 5. Number of nitrogens for each PEI and all PEIs within 4 Å of any N/O atom of the DNA as a function of time for systems D-4bP, D-4bP-S, D-4lP, and D-4lP-S.

DNA at all from the beginning. For example, PEI 6 in D-8lP-S does not make any close contact with the DNA during the entire simulation. PEI 8 in D-8lP and PEI 5 in D-8lP-S only have very few Ns in close contact with the DNAs for short periods. The large fluctuation for each PEI in systems D-8lP and D-8lP-S also reflects the intense competition for binding. Although there are more bP molecules bound with DNA than lPs, the number of all PEI Ns in close contact with the DNA is

dx.doi.org/10.1021/jp211716v | J. Phys. Chem. B 2012, 116, 2405–2413

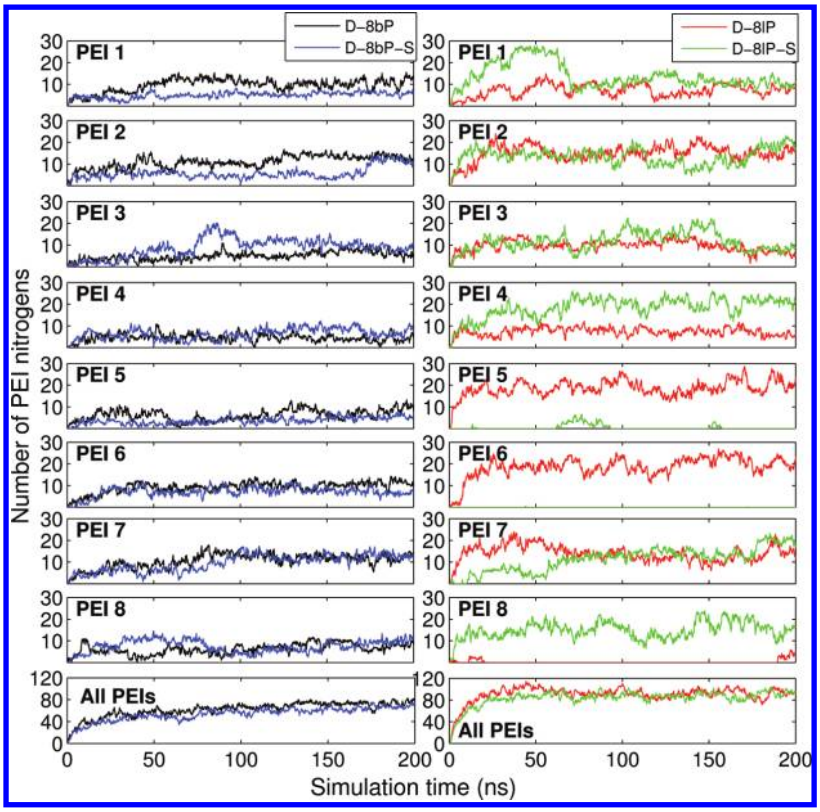

Figure 6. Number of nitrogens for each PEI and all PEIs within 4 Å of any N/O atom of the DNA as a function of time for systems D-8bP, D-8bP-S, D-8lP, and D-8lP-S.

still larger for the lPs. In particular, this number is ∼70 for D-8bP and D-8bP-S (equilibrated after 75 ns of the simulations) and ∼90 for D-8lP and D-8lP-S (equilibrated quickly after 25 ns of the simulations). This can be explained by the fact that the flexible lPs can better conformally coat the DNA, resulting in more intimate contact.

Table 2 summarizes the average numbers of the PEI Ns in close contact with the DNAs during the last 50 ns of the simulations. It can be seen at both DNA/PEI charge ratios, lPs have significantly more Ns in close contact with the DNAs than bPs, and when the charge ratio changes from 7/8 to 7/16 in all systems, the PEIs have 20−30 more Ns to establish close contact with the DNAs. At the charge ratio of 7/8, all PEIs bind to the DNA, and the complex formed by the DNA and 4 PEIs is positively charged with a net charge of +10. Despite this overall positive charge, when excess PEIs are present, they continue to bind to the DNA and the complexes formed by the DNA, and the 8 bPs or the 6 lPs represent significantly positively charged particles. The amine groups on the PEIs interact with the DNA N/O through direct or indirect hydrogen bonding,[21] and it is this local interaction that facilitates the continuing binding of the PEIs to the DNA. The stoppage of binding in the case of 8 lPs is unlikely driven by the positive charge of the complex since all 8 bPs bind to the DNA. Rather, it is driven by the fact that the entire DNA surface has been covered by the 6 lPs, prohibiting the local interaction of the other 2 lPs with the DNA. At zero and 154 mM salt concentrations, the numbers for D-4lP and D-4lP-S differ only by 0.2 Ns, and the difference between D-8lP and D-8lP-S is only 3 Ns. The less than 4% relative difference demonstrates that the salt ions have negligible effects on the binding of lPs to the DNA. This difference between D-4bP and D-4bP-S is 6.6 Ns and that between D-8bP and D-8bP-S is 7.1 Ns. This difference is relatively small (10−15% relative difference), but it also indicates that the salt ions have a stronger influence on the binding of bPs to the DNA.

Table 2. Average Numbers of the PEI Nitrogens in Close Contact with the DNAs during the Last 50 ns of the Simulations

system	D-4bP	D-4bP-S	D-8bP	D-8bP-S
number	50.9	44.3	72.7	65.6
system	D-4lP	D-4lP-S	D-8lP	D-8lP-S
number	74.6	74.4	92.7	89.7

The contribution of the PEI flexibility to binding can be further confirmed by examining the radius of gyration of the PEI molecules after the binding. R_g of each PEI in the complexation simulations is plotted in Figures S1 and S2 in the Supporting Information. In all cases, the bP maintains an almost constant R_g of ∼12 Å, nearly identical to the R_g value before the binding (see Figure 3). This implied that a bP undergoes little deformation as it binds to the DNA. On the contrary, smaller fluctuations in R_g was observed for the lP molecules after the binding, compared with the fluctuations before the binding (see Figure 3). This indicated that the lPs have conformed themselves to the DNA, lost some degrees of freedom and become less flexible. In addition, in systems D-8lP and D-8lP-S, the R_g values of the unbound PEIs (PEI 6 in D-8lP-S during the entire simulation; and PEI 8 in D-8lP and PEI 5 in D-8lP-S during most time of the simulations) fluctuated more than the bound PEIs, further confirming the ability of lPs to conform to the DNA upon binding.

dx.doi.org/10.1021/jp211716v | J. Phys. Chem. B 2012, 116, 2405−2413

Macromolecular association in solution can cause water molecules adhered to the surface of macromolecules to be released into the bulk solution. This process is entropically favorable since the water molecules on the macromolecular surface are less mobile.[33] Hence, counting the number of water molecules released from the macromolecules can give us an idea of the strength of interaction in terms of entropic gain from water release and changes in solution accessible surface area upon macromolecular binding. Figure 7 shows the number of water molecules in the hydration shell of the DNA or PEIs (within 3 Å from the molecules) as a function of simulation

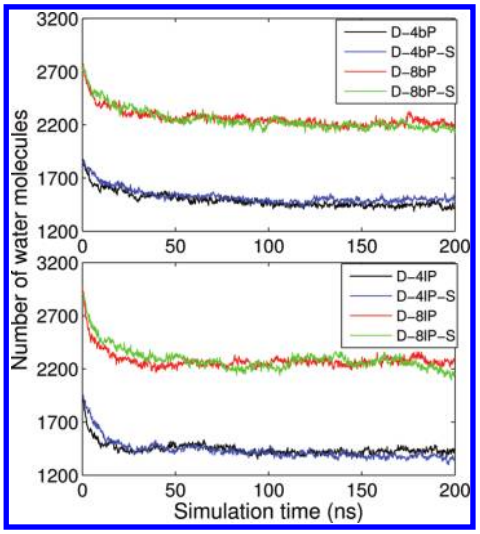

Figure 7. Number of water molecules in the hydration shell (within 3 Å of the DNA or PEIs) as a function of simulation time.

time. As the complexes form, the number of water molecules decreased concurrently, i.e., the water molecules were released from the macromolecules. It can be seen that lPs displaced more water molecules than bPs, with ∼500 released in D-4lP/D-4lP-S and ∼750 released in D-8lP/D-8lP-S, compared to ∼350 in D-4bP/D-4bP-S and ∼500 in D-8bP/D-8bP-S. Moreover, water release for lPs start to level off within 40 ns while it took them ∼100 ns to level off for the bPs. This again demonstrated the faster kinetics of DNA's complexation with lPs than with bPs due to the higher flexibility of the lP. Comparing Figure 7 with the subfigures of all PEIs in Figures 5 and 6, we found that the number of released water molecules correlates well with the number of PEI Ns in close contact with the DNA: with more PEI Ns coming into close contact with the DNA, more water molecules were released. At zero and 154 mM salt concentrations, the numbers of water molecules released for two systems with the same number and species of molecules are very close, confirming again that the 154 mM salt does not affect on the complexation of PEIs with the DNA to a significant degree.

3.3. Charge Neutralization. The simulation results clearly show that PEIs can bind with the DNA and form an overall positively charged particle to overneutralize the DNAs. In our previous MD work of 600 Da PEI mediated DNA aggregation,[34] we have demonstrated that the neutralization of the DNA charges by PEIs plays an important role in PEI mediated DNA aggregation.[34] When the PEI/DNA charge ratio is above 1/1, a DNA aggregate can be formed, and when the charge ratio is reduced to 1/4, the DNA aggregate becomes unstable and eventually breaks.[34] To investigate how 2 kDa PEIs neutralize the DNA charges, we plotted the cumulative distributions, with respect to the DNA C1′ atoms, of protonated PEI Ns, Na^+ ions, Cl^- ions, and the net charge of PEI and ions, averaged over the last 50 ns of the simulations (Figure 8). In each subfigure, the straight dashed black line indicates the total charge of the DNA (−70), and the blue solid curve indicates the total charge of PEI and ions within a given distance to their nearest DNA C1′ atoms. At the intersection of the black line and blue curve, the DNA charges are 100% neutralized by the PEIs and ions. For all the 8 systems, at larger distances beyond the intersection of the black line and blue curve, the PEI and ion charges exceed the DNA charges to some extent, and the DNA is overneutralized at such distances. Comparing the subfigures on the left column and the ones on the right, we found that charge neutralization (the solid blue line) in systems with 154 mM salt has a very similar characteristic as their counterparts with zero salt concentration. For systems D-4bP and D-4bP-S, the DNA charges are 100% neutralized at a distance of ∼13 Å from their C1′ atoms, and the DNA is slightly overneutralized beyond this distance. However, at the same charge ratio for linear PEIs in systems D-4lP and D-4lP-S, the four PEIs neutralize the DNA at a much shorter distance of ∼9 Å from the DNA C1′ atoms. This can be attributed to the high flexibility of the lPs that can comply more easily with the DNA, resulting in shorter separation of the PEI N^+ from the DNA. This is also consistent with our previous finding that lP has more number of Ns in close contact with the DNA.

At the DNA/PEI charge ratio of 7/16, the DNAs are all 100% neutralized at a distance of ∼8 Å from their C1′ atoms similar to the scenario for D-4lP and D-4lP-S, but the DNAs are significantly overneutralized beyond this distance, and the overneutralization can reach a maximum of ∼20%. The difference between bP and lP lies where the overneutralization reaches its maximum. For systems D-8bP and D-8bP-S, the maximum is located at ∼20 Å, while for systems D-8lP and D-8lP-S, the maximum is located at a much shorter distance of ∼12 Å. Comparing the PEI N^+ distribution in systems D-8bP and D-8bP-S with that in systems D-8lP and D-8lP-S (green dashed curves in Figure 8e−h), we found that in the cases of D-8bP and D-8bP-S, ∼85 PEI N+ are within 10 Å of the DNA C1′ atoms and ∼140 PEI N+ are within 20 Å of the DNA C1′ atoms, while the two numbers for D-8lP and D-8lP-S are ∼90 and ∼110, respectively. Clearly the bP charges are located further away from the DNA. This once again can be explained by the higher flexibility of lP and the resulting more intimate binding structure compared with bP. If we define the charge center of a PEI as $(\sum_{i=1}^{N} q_i r_i / \sum_{i=1}^{N} q_i)$, where q_i is the charge of atom i, r_i is its location, and the summation is over all the N atoms in the PEI, then in binding with a DNA, the bPs have their charge centers located further from the DNA axis compared with lPs.

On the basis of the analyses of sections 3.2 and 3.3, we revealed distinct modes of bP and lP binding with DNAs. A bP tends to have a part of the molecule in close contact with the DNA and leaves the remaining part outward. In the scenario of one DNA segment with multiple bPs, the bPs resemble beads adhering on the surface of the DNA, with their overall charge center located further from the DNA axis compared with that of lPs. The lPs tend to adhere on the DNA surface like cords; because of the high flexibility, the overall charge center of lPs are closer to the DNA axis than that of the bPs. The different binding mode of bP and lP with DNA can affect how the PEIs

dx.doi.org/10.1021/jp211716v | J. Phys. Chem. B 2012, 116, 2405−2413

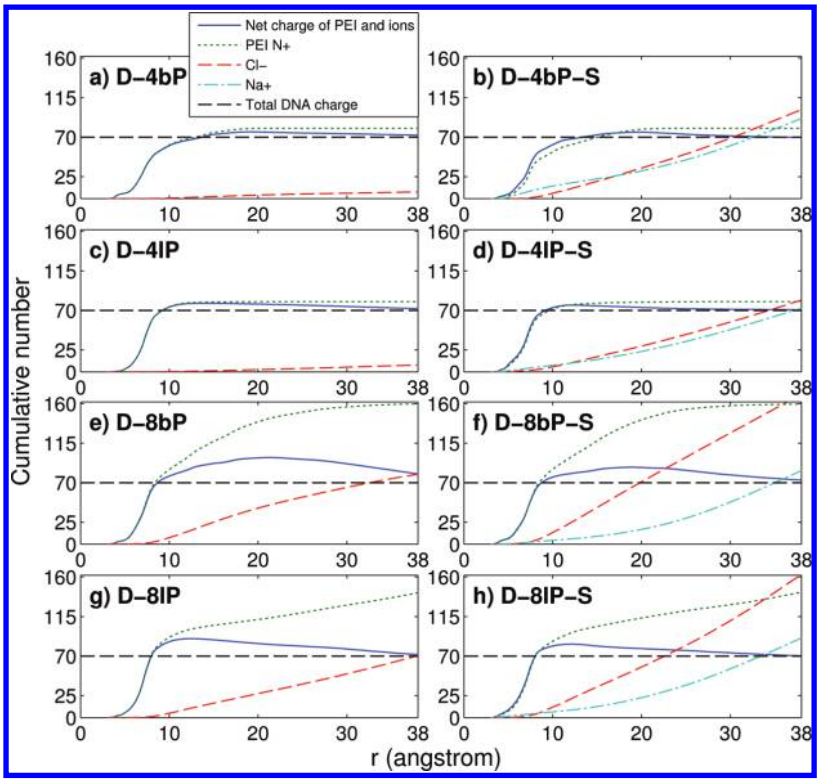

Figure 8. Cumulative numbers of protonated PEI nitrogens, Na^+, Cl^-, and net charge of PEI/Na+/Cl^- as a function of the distance from any C1′ DNA atom, averaged over the last 50 ns of each simulation. The total charge of the DNA in each system is plotted by straight dashed black lines as a reference. (a) D-4bP, (b) D-4bP-S, (c) D-4lP, (d) D-4lP-S, (e) D-8bP, (f) D-8bP-S, (g) D-8lP, and (h) D-8lP-S.

contribute to DNA aggregation, i.e., when they mediate the condensation of plasmid DNAs. The lP molecules bind very tightly to one DNA segment, leaving little room for interaction with other DNA segments. In addition, for the same amount of molecules, lPs provide better surface coverage of the DNA, the net result being that fewer lPs can bind to the DNA segment and serve as polyion bridges in DNA aggregation. On the contrary, the outward bP moiety might facilitate the PEIs to attract other DNA segments to form more stable DNA/PEI nanoparticles. The different binding modes of lP and bP elucidated here provide a mechanistic explanation to the experimental finding that bP forms more stable nanoparticles with DNA, while lP has a better capacity to unload DNA inside cells.[13,15]

In our previous study of the complexation between single 600 Da PEI and DNA,[21] we did not find that the architecture of PEIs had a profound effect on DNA binding, in that four PEIs of different degrees of branching had a similar number of Ns in close contact with DNA. Specifically, at the same protonation ratio of 46%, a linear 600 Da PEI has an average number of 6.2 Ns in close contact with the DNA N/O, while a highly branched 600 Da PEI has an average number of 5.5 Ns in close contact with the DNA N/O. So, the difference is about 0.7 Ns per PEI. If we have 12 600 Da PEIs complexing with the DNA (total molecular weight similar to four PEIs in this study), then the difference will be about 8.4 Ns, and for 24 600 Da PEIs complexing with the DNA (total molecular weight similar to eight PEIs in this study), the difference will be about 16.8 Ns. However, the difference observed for the 2 kDa linear and branched PEIs is much larger, being 20−30 Ns in the case of 4 PEIs complexing with the DNA. In the case of 8 PEIs complexing with the DNA, all the branched PEIs bind to the DNA, while only 6 out of the 8 linear PEIs bind to the DNA. Nevertheless, the number of Ns in close contact with the DNA in the case of linear PEI still exceeds the case of branched PEI by more than 20. Clearly, the effect of PEI architecture manifests differently for different PEI sizes. At 600 Da, the branched PEIs have short branches; hence, the steric hindrance that each branch experiences in binding with DNA is rather small, and as a result, the branched 600 Da PEI binds to DNA in a similar way as a linear 600 Da PEI. The 2 kDa branched PEIs have more and longer branches so that the dendritic nature of PEI gives greater steric hindrance for amines in binding to DNA, which can explain the distinctly different binding mode it displays compared with that of linear PEIs.

The influence of the molecular weight of PEIs is also reflected in the neutralizing distance for the DNA. In excess of PEIs, both 2 kDa bP and lP fully neutralize the DNA at a distance of ∼8 Å from the DNA C1′ atoms, which is significantly shorter compared with ∼12 Å at which the 600 Da branched PEIs fully neutralize the DNA.[34] This implies that 2 kDa PEIs might form nanoparticles with higher DNA density compared with 600 Da PEIs, which can further facilitate the membrane transfer and better protect DNA from degradation on the delivery route.

4. CONCLUSIONS

We performed a series of all-atom MD simulations to study the complexation of DNA with 2 kDa branched and linear PEIs. The results revealed the distinct modes of bP and lP in binding to DNA. The bPs bound to DNA like beads adhering to the DNA surface, with little deformation upon binding. The lPs were very flexible and bound to DNA like cords conforming to the DNA surface. The tighter binding of lPs with DNA results

dx.doi.org/10.1021/jp211716v | J. Phys. Chem. B 2012, 116, 2405−2413

in the overall charge center of the lPs being located closer to the DNA axis. In particular, at a PEI/DNA charge ratio of close to 1 (8/7), bP and lP fully neutralized the DNA at ∼13 Å and ∼9 Å from the DNA C1′ atoms, respectively. The tighter binding of lPs further causes more water to be displaced and potentially leads to energetically more stable DNA−lPs complexes. On the other hand, the lPs provide better surface coverage of the DNA, which limits the number of lPs that can complex with the DNA and the interaction of lPs with multiple DNAs. This can have a negative effect on DNA aggregation needed for cell uptake.

Compared with the results for 2 kDa PEIs, previous work on 600 Da PEIs did not show such significant dependence on PEI architecture. This demonstrates that molecular weight of PEI is an important factor in DNA/PEI complexation. Further evidence for this exists in the fact that in excess of PEIs at a PEI/DNA charge ratio of 16/7, both bP and lP fully neutralized the DNA at a distance of ∼8 Å from the DNA C1′ atoms, which is a significantly shorter distance compared with ∼12 Å in the case of excessive 600 Da PEIs. Finally, our simulations in both physiological and zero-salt conditions showed that the presence of salt had a small effect on DNA/PEI complexation, with a slightly larger influence on the bP molecules.

■ ASSOCIATED CONTENT

Supporting Information

Radius of gyration of each PEI as a function of simulation time in each system. This material is available free of charge via the Internet at http://pubs.acs.org.

■ AUTHOR INFORMATION

Corresponding Author

*Phone: +1-780-492-5467. Fax: +1-780-492-2200. E-mail: tian.tang@ualberta.ca.

Notes

The authors declare no competing financial interest.

■ ACKNOWLEDGMENTS

We acknowledge the computing resources and technical support from the high performance computing facility at the National Institute for Nanotechnology, Edmonton, Canada. This work was supported by the National Science and Engineering Research Council of Canada, Alberta Innovates Technology Futures, and Canada Foundation for Innovation.

■ REFERENCES

(1) Ledley, F. *Hum. Gene Ther.* **1995**, *6*, 1129−1144.
(2) Luo, D.; Saltzman, W. *Nat. Biotechnol.* **2000**, *18*, 33−37.
(3) Boussif, O.; Lezoualc'h, F.; Zanta, M. A.; Mergny, M. D.; Scherman, D.; Demeneix, B.; Behr, J. P. *Proc. Natl. Acad. Sci. U.S.A.* **1995**, *92*, 7297−7301.
(4) Godbey, W.; Wu, K.; Mikos, A. *J. Controlled Release* **1999**, *60*, 149−160.
(5) Godbey, W.; Wu, K.; Mikos, A. *J. Biomed. Mater. Res.* **1999**, *45*, 268−275.
(6) Wightman, L.; Kircheis, R.; Rossler, V.; Carotta, S.; Ruzicka, R.; Kursa, M.; Wagner, E. *J. Gene Med.* **2001**, *3*, 362−372.
(7) Bahadur, K. C. R.; Landry, B.; Aliabadi, H. M.; Lavasanifar, A.; Uludag, H. *Acta Biomater.* **2011**, *7*, 2209−2217.
(8) Aliabadi, H. M.; Landry, B.; Bahadur, R. K.; Neamnark, A.; Suwantong, O.; Uludag, H. *Macromol. Biosci.* **2011**, *11*, 662−672.
(9) Jere, D.; Jiang, H. L.; Arote, R.; Kim, Y. K.; Choi, Y. J.; Cho, M. H.; Akaike, T.; Chot, C. S. *Expert Opin. Drug Delivery* **2009**, *6*, 827−834.
(10) Neamnark, A.; Suwantong, O.; Bahadur, R. K. C.; Hsu, C. Y. M.; Supaphol, P.; Uludag, H. *Mol. Pharmaceutics* **2009**, *6*, 1798−1815.
(11) Hsu, C. Y. M.; Hendzel, M.; Uludag, H. *J. Gene Med.* **2011**, *13*, 46−59.
(12) Wiseman, J.; Goddard, C.; McLelland, D.; Colledge, W. *Gene Ther.* **2003**, *10*, 1654−1662.
(13) Itaka, K.; Harada, A.; Yamasaki, Y.; Nakamura, K.; Kawaguchi, H.; Kataoka, K. *J. Gene Med.* **2004**, *6*, 76−84.
(14) Intra, J.; Salem, A. K. *J. Controlled Release* **2008**, *130*, 129−138.
(15) Dai, Z.; Gjetting, T.; Mattebjerg, M. A.; Wu, C.; Andresen, T. L. *Biomaterials* **2011**, *32*, 8626−8634.
(16) Ziebarth, J.; Wang, Y. *Biophys. J.* **2009**, *97*, 1971−1983.
(17) Pavan, G. M.; Danani, A.; Pricl, S.; Smith, D. K. *J. Am. Chem. Soc.* **2009**, *131*, 9686−9694.
(18) Pavan, G. M.; Albertazzi, L.; Danani, A. *J. Phys. Chem. B* **2010**, *114*, 2667−2675.
(19) Pavan, G. M.; Kostiainen, M. A.; Danani, A. *J. Phys. Chem. B* **2010**, *114*, 5686−5693.
(20) Pavan, G. M.; Mintzer, M. A.; Simanek, E. E.; Merkel, O. M.; Kissel, T.; Danani, A. *Biomacromolecules* **2010**, *11*, 721−730.
(21) Sun, C.; Tang, T.; Uludag, H.; Cuervo, J. E. *Biophys. J.* **2011**, *100*, 2754−2763.
(22) Boeckle, S.; von Gersdorff, K.; van der Piepen, S.; Culmsee, C.; Wagner, E.; Ogris, M. *J. Gene Med.* **2004**, *6*, 1102−1111.
(23) Case, D. et al. *AMBER 10*; University of California: San Francisco, CA, 2008.
(24) Utsuno, K.; Uludag, H. *Biophys. J.* **2010**, *99*, 201−207.
(25) Brooks, B.; Bruccoleri, R.; Olafson, D.; States, D.; Swaminathan, S.; Karplus, M. *J. Comput. Chem.* **1983**, *4*, 187−217.
(26) MacKerel, A. Jr.; Brooks, C. III; Nilsson, L.; Roux, B.; Won, Y.; Karplus, M. In *CHARMM: The Energy Function and Its Parameterization with an Overview of the Program*; The Encyclopedia of Computational Chemistry; Schleyer,v. R., et al., Eds.; John Wiley & Sons: Chichester, U.K., 1998; Vol. *1*, pp 271−277.
(27) Vanommeslaeghe, K.; Hatcher, E.; Acharya, C.; Kundu, S.; Zhong, S.; Shim, J.; Darian, E.; Guvench, O.; Lopes, P.; Vorobyov, I.; MacKerell, A. D. Jr. *J. Comput. Chem.* **2010**, *31*, 671−690.
(28) Phillips, J.; Braun, R.; Wang, W.; Gumbart, J.; Tajkhorshid, E.; Villa, E.; Chipot, C.; Skeel, R.; Kale, L.; Schulten, K. *J. Comput. Chem.* **2005**, *26*, 1781−1802.
(29) Jorgensen, W. *J. Am. Chem. Soc.* **1981**, *103*, 335−340.
(30) Darden, T.; York, D.; Pedersen, L. *J. Chem. Phys.* **1993**, *98*, 10089−10092.
(31) Ryckaert, J.; Ciccotti, G.; Berendsen, H. *J. Comput. Phys.* **1977**, *23*, 327−341.
(32) Humphrey, W.; Dalke, A.; Schulten, K. *J. Mol. Graphics* **1996**, *14*, 33−38.
(33) Dunitz, J. *Science* **1994**, *264*, 670.
(34) Sun, C.; Tang, T.; Uludag, H. *Biomacromolecules* **2011**, *12*, 3698−3707.